

## CHAPTER IV

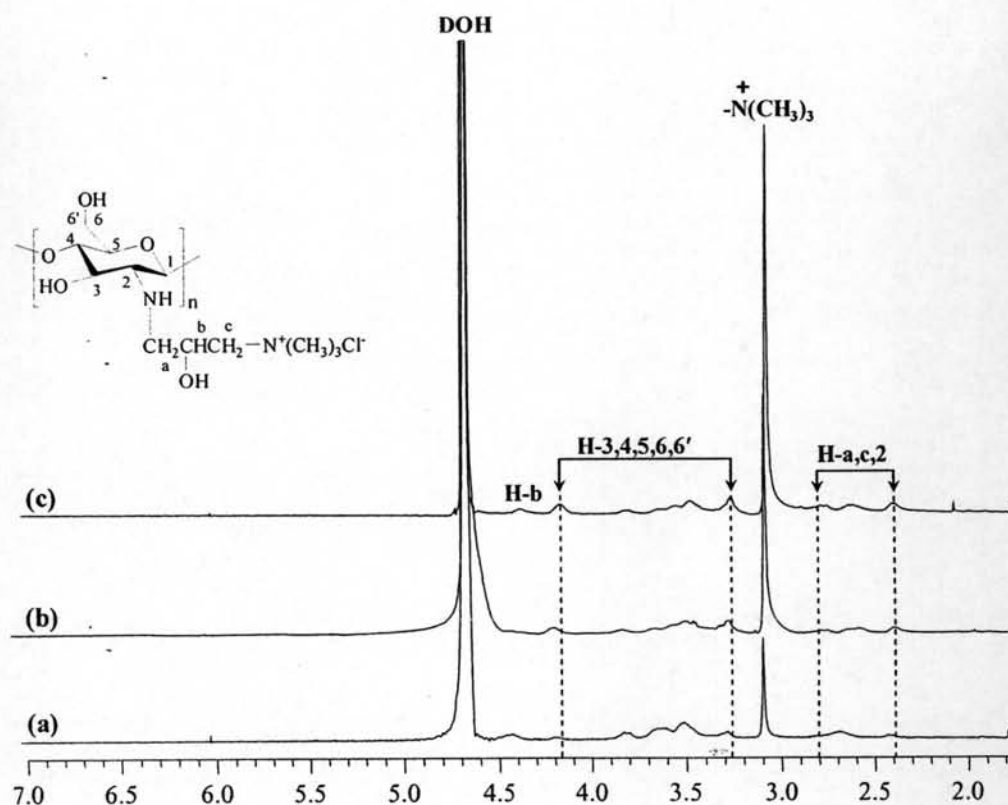
### RESULTS AND DISCUSSION

This chapter was divided into 3 parts. The first part concentrated on the synthesis and characterization of positively charged chitosan, *N*-[(2-hydroxyl-3-trimethylammonium)propyl]chitosan chloride (HTACC) and negatively charged chitosan, *N*-succinyl chitosan (SCC) and *N*-sulfofurfuryl chitosan (SFC). The ability of HTACC, SCC and SFC to form multilayer thin film was determined and explained in the second part. The last part was dedicated to the evaluation of cellular response of the assembled multilayer films having different numbers of deposition and charge.

#### 4.1 Synthesis and Characterization of Charged Derivatives of Chitosan

##### 4.1.1 Synthesis of *N*-[(2-hydroxyl-3-trimethylammonium)propyl]chitosan chloride (HTACC)

*N*-[(2-hydroxyl-3-trimethylammonium)propyl]chitosan chloride or HTACC, the positively charged derivative of chitosan was synthesized by epoxide ring opening of glycidyltrimethylammonium chloride (GTMAC) (Scheme 2.3 in Chapter 2) by amino groups of chitosan under acidic condition. In theory, GTMAC mainly reacts with amino (NH<sub>2</sub>) groups under acidic condition but preferably reacts with hydroxyl (OH) groups under neutral and alkaline conditions. The acidic condition causes protonation at the oxygen atom and makes the epoxy ring of GTMAC more reactive towards the NH<sub>2</sub> groups of chitosan. Figure 4.1 illustrates <sup>1</sup>H NMR spectra of the synthesized HTACC. Signals corresponding to the protons of CH<sub>2</sub> and CH appeared at 2.6 and 4.4 ppm, respectively. Furthermore, there is a new strong peak of CH<sub>3</sub> at 3.1 ppm, indicating that the quaternary ammonium group of N<sup>+</sup>(CH<sub>3</sub>)<sub>3</sub> were incorporated.



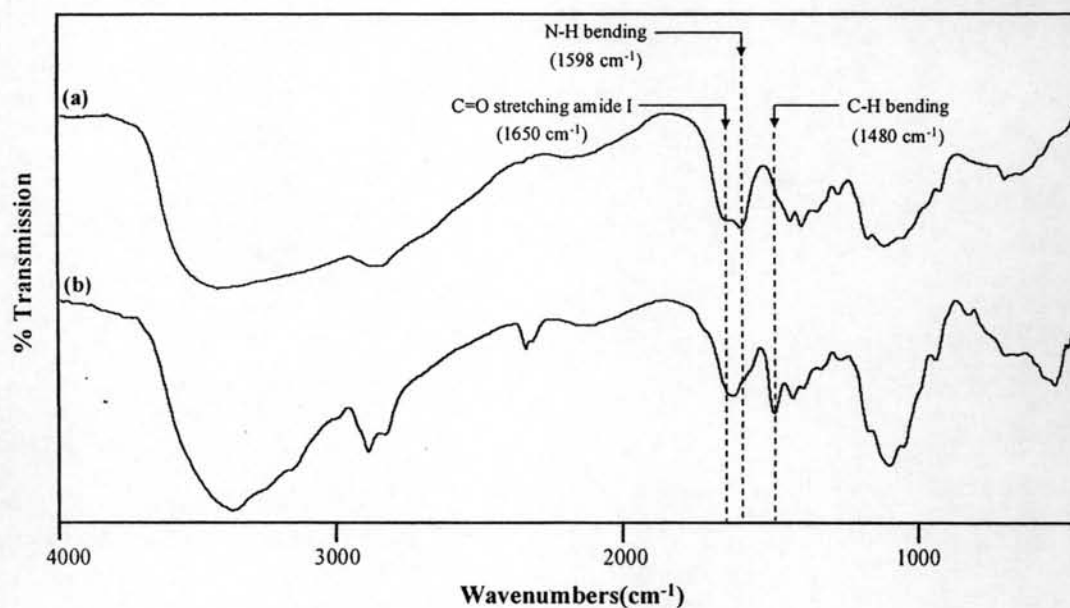
**Figure 4.1**  $^1\text{H}$  NMR spectra of HTACC obtained using (a) 2, (b) 4, and (c) 6 equivalents of GTMAC in comparison with the  $\text{NH}_2$  of chitosan (solvent:  $\text{D}_2\text{O}$ ,  $25^\circ\text{C}$ ).

Percentage of the degree of substitution (%DS) of GTMAC on chitosan was calculated from the relative ratio between the peak integration of protons from the quaternary ammonium group at 3.1 ppm of GTMAC and the sum of integral intensities of H-3,4,5,6 and 6' ( $\delta$  3.3- 4.3 ppm) from chitosan. From Table 4.1, the %DS of quaternary ammonium group on chitosan was drastically increased from 27 to 105 when the GTMAC equivalent was increased from 2 to 6. The %DS was not much increased when using 6 equivalents of GTMAC, 4 equivalents of GTMAC was therefore suggested as the optimal ratio for the preparation of HTACC to be used for multilayer assembly.

**Table 4.1** Degree of substitution (%DS) of quaternary ammonium group on chitosan after reacting with GTMAC at 70 °C in 1.0 % (v/v) acetic acid for 24 h as determined by  $^1\text{H}$  NMR.

| Equivalent of GTMAC | %DS |
|---------------------|-----|
| 2                   | 27  |
| 4                   | 94  |
| 6                   | 105 |

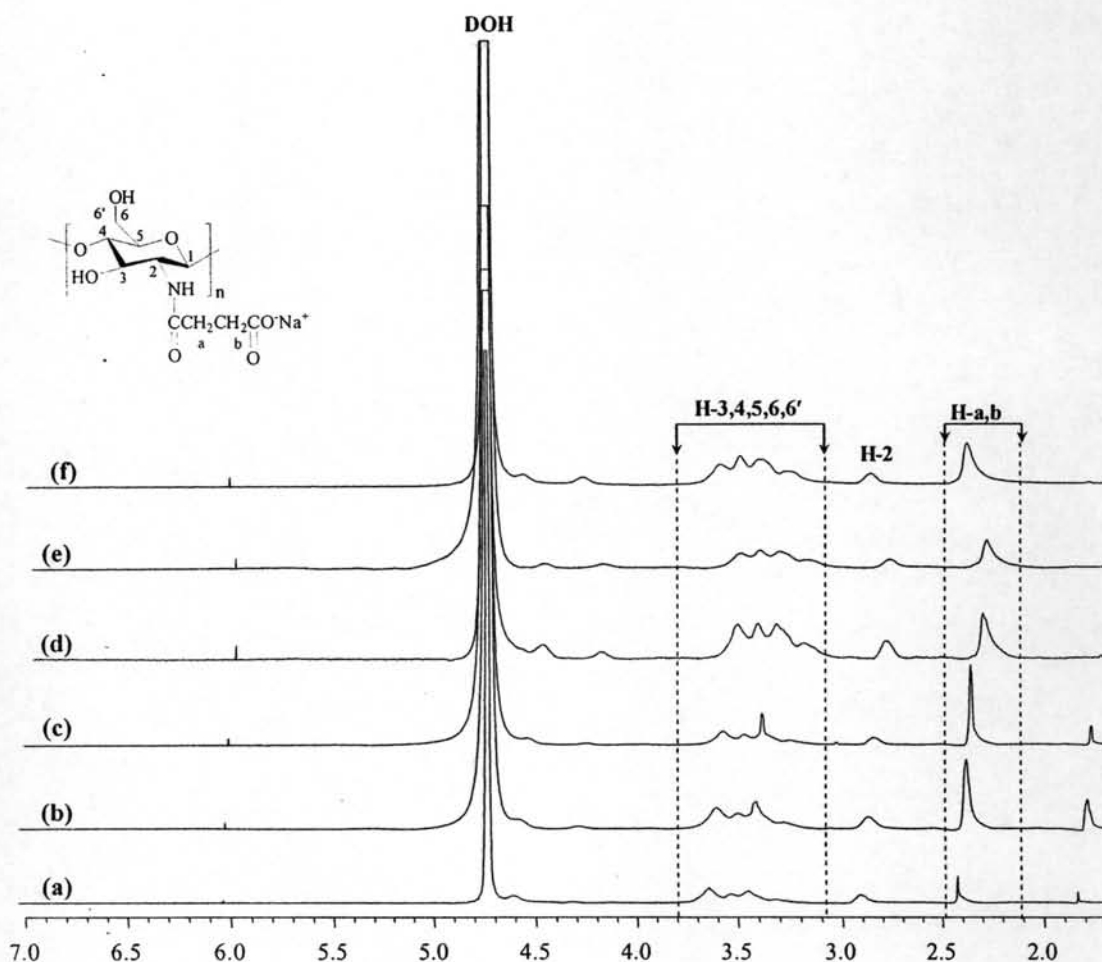
The success of HTACC synthesis could also be verified by the decrement of the N-H scissoring peak at  $1598\text{ cm}^{-1}$  of amino groups of chitosan and the appearance of C-H bending peak at  $1480\text{ cm}^{-1}$  corresponding to the methyl groups of quaternary ammonium groups as shown in Figure 4.2.



**Figure 4.2** FTIR spectra of (a) CHI and (b) HTACC.

#### 4.1.2 Synthesis of *N*-succinyl chitosan (SCC)

*N*-succinyl chitosan (SCC), one of the negatively charged derivatives of chitosan was synthesized by a ring opening reaction of succinic anhydride (SA) (Scheme 2.5 in Chapter 2) by the amino groups ( $\text{NH}_2$ ) of chitosan in aqueous methanol system at room temperature.  $^1\text{H}$  NMR signals of two succinyl protons at 2.2-2.5 ppm in Figure 4.3 confirmed the attachment of succinyl group to the chitosan backbone. The %DS of the succinyl group was determined from the relative ratio between the peak integration of four protons from succinyl moiety and the peak integration of five protons of chitosan ( $\delta$  3.0- 3.8 ppm).



**Figure 4.3**  $^1\text{H}$  NMR spectra of SCC obtained using (a) 1, (b) 2, (c) 3, (d) 4, (e) 8, and (f) 12 equivalents of SA in comparison with the  $\text{NH}_2$  of chitosan (solvent:  $\text{D}_2\text{O}/\text{TFA}$ ,  $25^\circ\text{C}$ ).

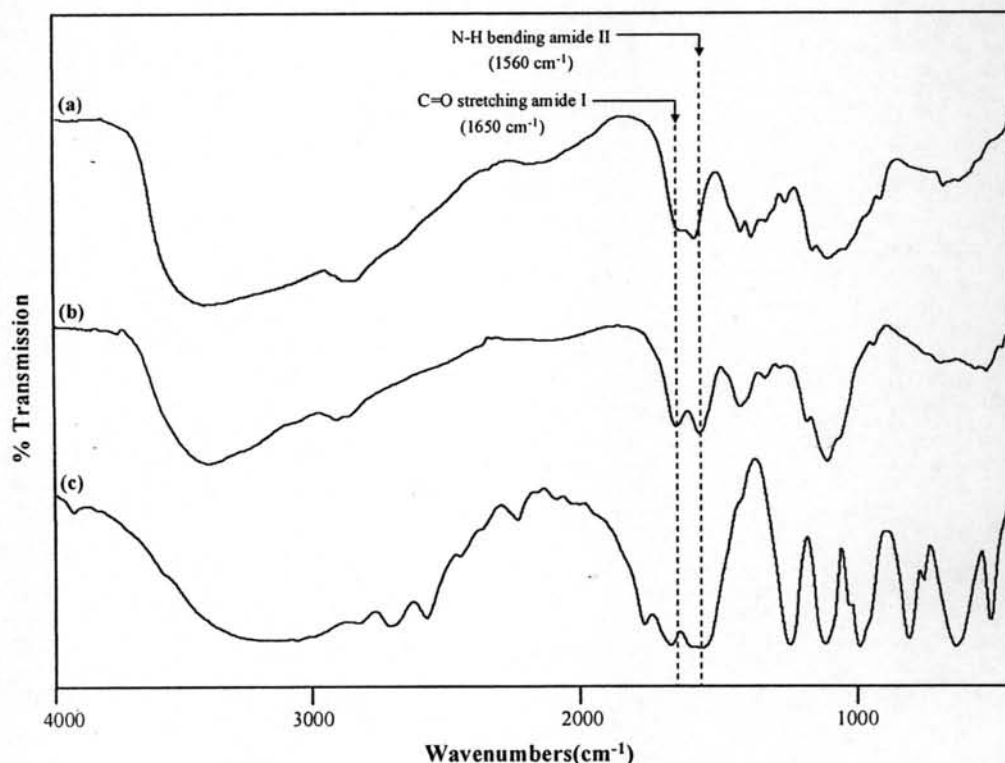
According to Table 4.2, the %DS of SCC increased with the amount of SA. The %DS, using 4 equivalents of SA, was 44. The %DS was not much increased when using 8 to 12 equivalents of SA, 4 equivalents of SA was therefore suggested as the optimal ratio for the preparation of SCC to be used for multilayer assembly. The kinetic studies (the data not shown) also suggest that 2 h be certainly enough for the substitution of SA to reach the highest extent.

**Table 4.2** Degree of substitution (%DS) of succinyl group on chitosan after reacting with SA in 1.0 % (v/v) acetic acid for 2 h as determined by  $^1\text{H}$  NMR.

| Equivalent of SA | %DS |
|------------------|-----|
| 1                | 17  |
| 2                | 27  |
| 3                | 36  |
| 4                | 44  |
| 8                | 46  |
| 12               | 47  |

The chemical structure of SCC was confirmed by FTIR analysis. The IR spectrum of chitosan and SCC are displayed in Figure 4.4. For chitosan, there should be three characteristic peaks in a region of  $1500\text{--}1700\text{ cm}^{-1}$ . One at  $1650\text{ cm}^{-1}$  corresponds to C=O stretching (amide I peak). Other two peaks are at  $1598\text{ cm}^{-1}$  and  $1560\text{ cm}^{-1}$  which correspond to N-H bending of amino group and N-H bending (amide II) of amide group. Due to the signal overlapping of all three peaks, the one in the middle (at  $1598\text{ cm}^{-1}$ ) cannot be separately identified. As a consequence of succinyl group substitution and the formation of additional amide linkages, the signal due to N-H bending of amino group was correspondingly decreased whereas the signals of both amide I and amide II increased. These explained why the signal of amide I and amide II in the SCC spectrum was better separated. The increment of the amide I peak ( $1650\text{ cm}^{-1}$ ), the amide II peak ( $1560\text{ cm}^{-1}$ ), and the decrease of the

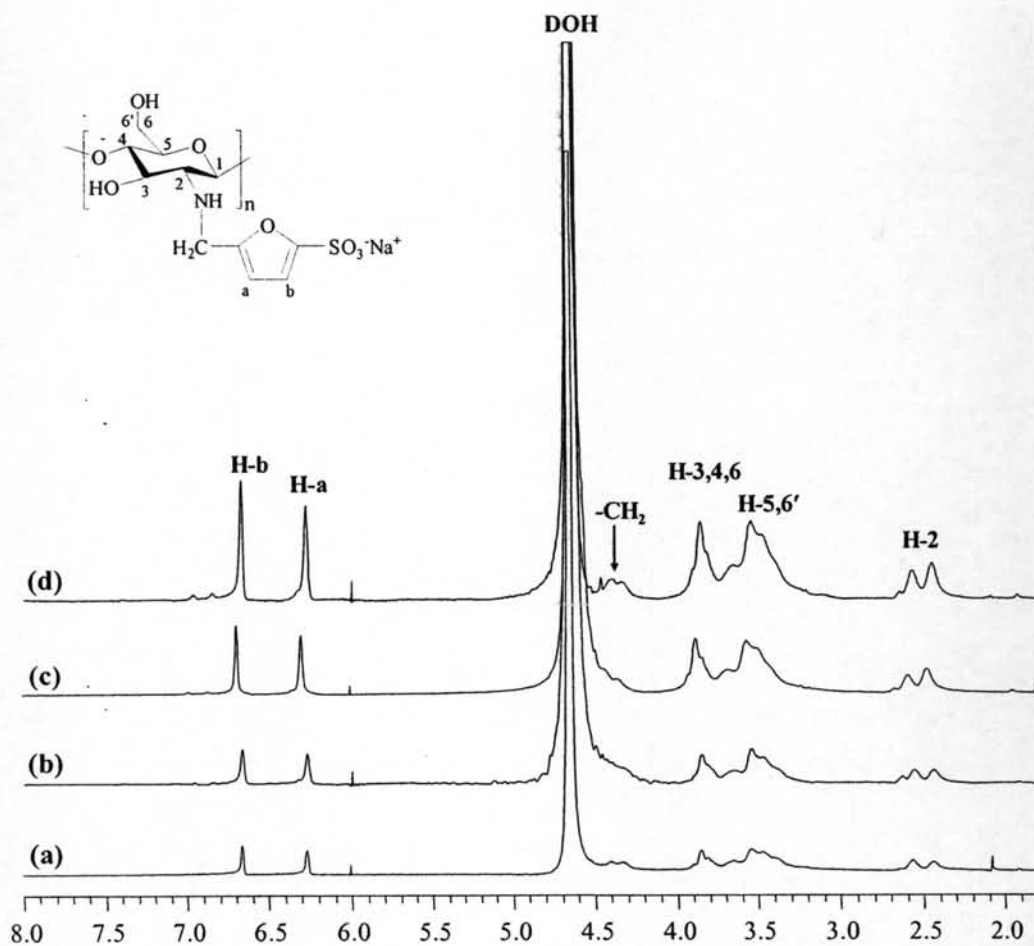
amino group ( $1598\text{ cm}^{-1}$ ) indicated a greater extent of amidation by the reaction between chitosan and succinic anhydride.



**Figure 4.4** FTIR spectra of (a) CHI, (b) SCC, and (c) SA.

#### 4.1.3 Synthesis of *N*-sulfofurfuryl chitosan (SFC)

*N*-sulfofurfuryl chitosan or SFC, the other negatively charged derivative of chitosan, was synthesized by reductive alkylation (Scheme 2.7 in Chapter 2) between the amino groups ( $\text{NH}_2$ ) of chitosan and 5-formyl-2-furansulfonic acid, sodium salt (FFSA) at room temperature *via* Schiff's base under mild condition.  $^1\text{H}$  NMR signals of the two furan protons at 6.3 and 6.7 ppm in Figure 4.5 confirmed the attachment of the heterocyclic component. Furthermore, there was a new signal appearing approximately at 4.4 ppm corresponding to the two protons of methylene group that links between the amino group of chitosan and the furan ring. However, the signal could not be clearly observed when the low equivalent of FFSA to the amino groups was used.



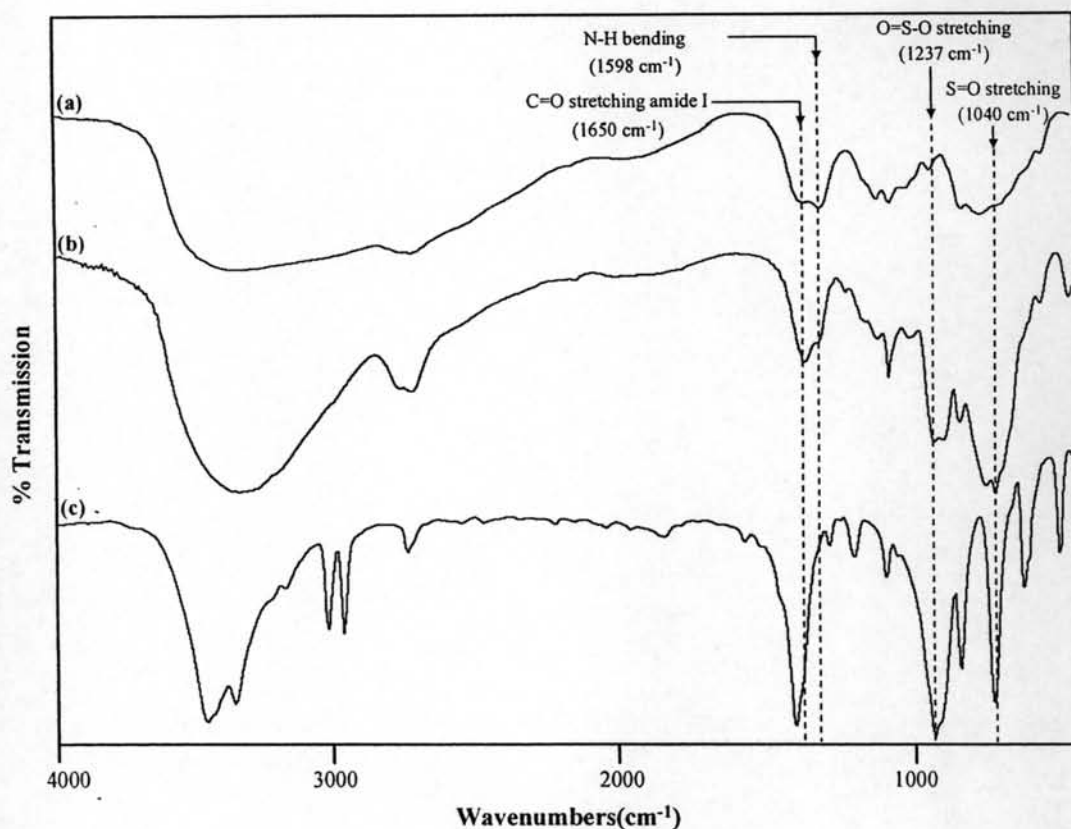
**Figure 4.5**  $^1\text{H}$  NMR spectra of SFC obtained using (a) 0.5, (b) 1, (c) 2, and (d) 4 equivalents of FFSA in comparison with the  $\text{NH}_2$  of chitosan (solvent:  $\text{D}_2\text{O}$ ,  $25^\circ\text{C}$ ).

The %DS of sulfonate group can be determined by the relative ratio between the peak integration of the two protons of furan group and the peak integration of five protons of chitosan (chemical shift 3.0-3.8 ppm). From Table 4.3, the %DS of sulfonate group on chitosan was apparently elevated from 32 to 66 when the FFSA equivalent was increased from 0.5 to 4. %DS was not much further increased using 4 equivalent of FFSA, therefore, 2 equivalents of FFSA was suggested as the optimal ratio for the preparation of SFC to be used for multilayer assembly.

**Table 4.3** Degree of substitution (%DS) of sulfonate group on chitosan after reacting with FFSA in acetic acid/MeOH (1:1, v/v) for 18 h as determined by  $^1\text{H}$  NMR.

| Equivalent of FFSA | %DS |
|--------------------|-----|
| 0.5                | 32  |
| 1                  | 50  |
| 2                  | 64  |
| 4                  | 66  |

As shown in Figure 4.6, the appearance of peaks at  $1237\text{ cm}^{-1}$  of O=S-O stretching and  $1040\text{ cm}^{-1}$  of S=O stretching in the spectrum of SFC signified the presence of the sulfonate salt and sulfonic acid functionality, respectively.



**Figure 4.6** FTIR spectra of (a) CHI, (b) SFC, and (c) FFSA.



#### 4.1.4 Solubility of Charged Derivatives of Chitosan

The solubility test was performed according to a method of Sashiwa *et al.* [22]. The solid sample of charged derivative of chitosan (60 mg) was dissolved in water (20 mL). The pH of the solution was adjusted with 1.0% w/v aqueous HCl and NaOH. The synthesized HTACC, SCC and SFC showed the solubility in the opposite pH range to the virgin chitosan. As illustrated in Table 4.4, chitosan which is the starting material in this study, dissolved only in acidic region below pH 6.5. The solubility of chitosan in the acidic region is ascribed to the protonation of amino group (from  $-\text{NH}_2$  to  $-\text{NH}_3^+$ ). In contrast, HTACC having quaternary ammonium groups showed the solubility in the entire pH range. SCC with the %DS higher than 44% was insoluble in acidic and neutral regions between pH 3.5-7.0. The solubility in acidic region below 3.5 would be explained by the protonation of the unsubstituted amino group (from  $-\text{NH}_2$  to  $-\text{NH}_3^+$ ). The solubility in alkaline region would be due to the change of carboxyl group to carboxylate ion (from  $-\text{COOH}$  to  $-\text{COO}^-$ ). The insolubility in the range of pH 3.5-7.0 may possibly be owing to the isoelectric point at which equimolar of  $-\text{NH}_3^+$  and  $-\text{COO}^-$  groups exists in the molecule. Having the %DS lower than 44%, SCC exhibited the solubility in different pH ranges, more or less similar to chitosan. SFC showed the solubility only in the alkaline region range (pH 8-13), and the insolubility in acidic (pH < 7) and neutral region (pH 7). It should also be noted that increasing the %DS from 32 to 66% did not affect the solubility range of SFC.

**Table 4.4** Solubility test of CHI, HTACC, SCC, and SFC in water of various pHs<sup>a</sup>

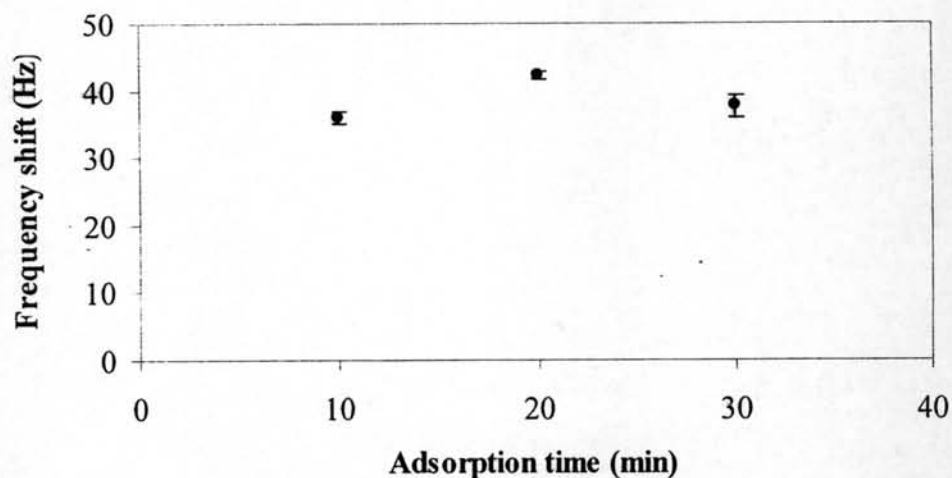
| Sample | Solubility <sup>b</sup> |   |   |   |   |   |   |   |   |   |    |    |    |    |
|--------|-------------------------|---|---|---|---|---|---|---|---|---|----|----|----|----|
|        | pH:                     | 1 | 2 | 3 | 4 | 5 | 6 | 7 | 8 | 9 | 10 | 11 | 12 | 13 |
| CHI    |                         |   |   |   |   |   |   |   |   |   |    |    |    |    |
| HTACC  |                         |   |   |   |   |   |   |   |   |   |    |    |    |    |
| SCC    |                         |   |   |   |   |   |   |   |   |   |    |    |    |    |
| SFC    |                         |   |   |   |   |   |   |   |   |   |    |    |    |    |

<sup>a</sup>The solid sample (60 mg) was dispersed in H<sub>2</sub>O (20 mL). The pH of solution was adjusted with 1% aqueous HCl and NaOH.

<sup>b</sup>White bar = soluble, black bar = insoluble

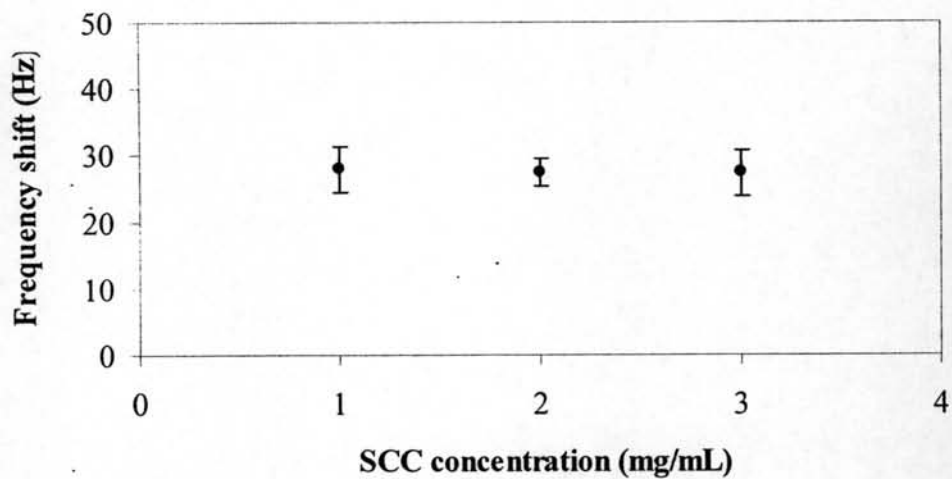
#### 4.1.5 Adsorption of Charged Derivatives of Chitosan

To select the adsorption time at which adsorption of SCC (44 %DS) has reached its equilibrium, the conventional mode of adsorption was operated using QCM measurement. Figure 4.7 shows a frequency shift of quartz plate due to SCC adsorption. The greatest frequency shift of the quartz was observed when the adsorption proceeded for 20 min; the later period of time was used for multilayer assembly. It should be underlined that the adsorption time of 20 min used for the assembly of other two derivatives: SFC and HTACC was selected based on the optimization previously done by Channasanon and co-workers [12].

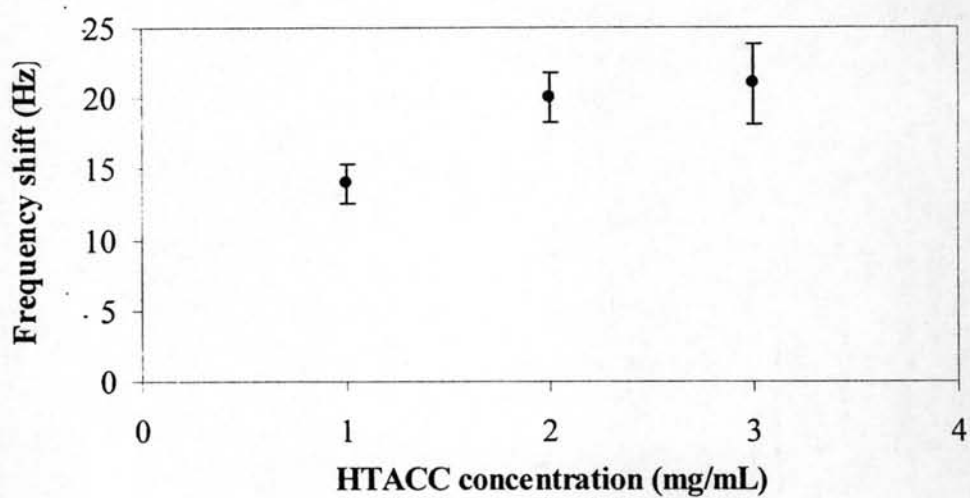


**Figure 4.7** Frequency shift of the quartz plate upon the adsorption of 2 mg/mL SCC as a function of adsorption time as determined by QCM using the conventional mode.

To select the optimal concentration that the adsorption of SCC (44 %DS) and HTACC (78 %DS) have reached their equilibrium, the conventional mode of QCM analysis was performed. Figure 4.8 shows frequency shifts of the quartz crystal due to SCC adsorption. As the concentration increased, the frequency shift was not significantly varied. The concentration of 1 mg/mL seemed to be sufficient for the SCC adsorption to reach its equilibrium. This concentration was then later used for multilayer assembly. Unlike SCC, the concentration of as high as 2 mg/mL was necessary for the adsorption of HTACC to reach its equilibrium (Figure 4.9). As reported by Channasanon *et al.*, the optimal concentration for the adsorption of HTACC (96 %DS) was 3 mg/mL.



**Figure 4.8** Frequency shift of the quartz plate upon the adsorption of SCC for 20 min as a function of SCC concentration as determined by QCM using the conventional mode.

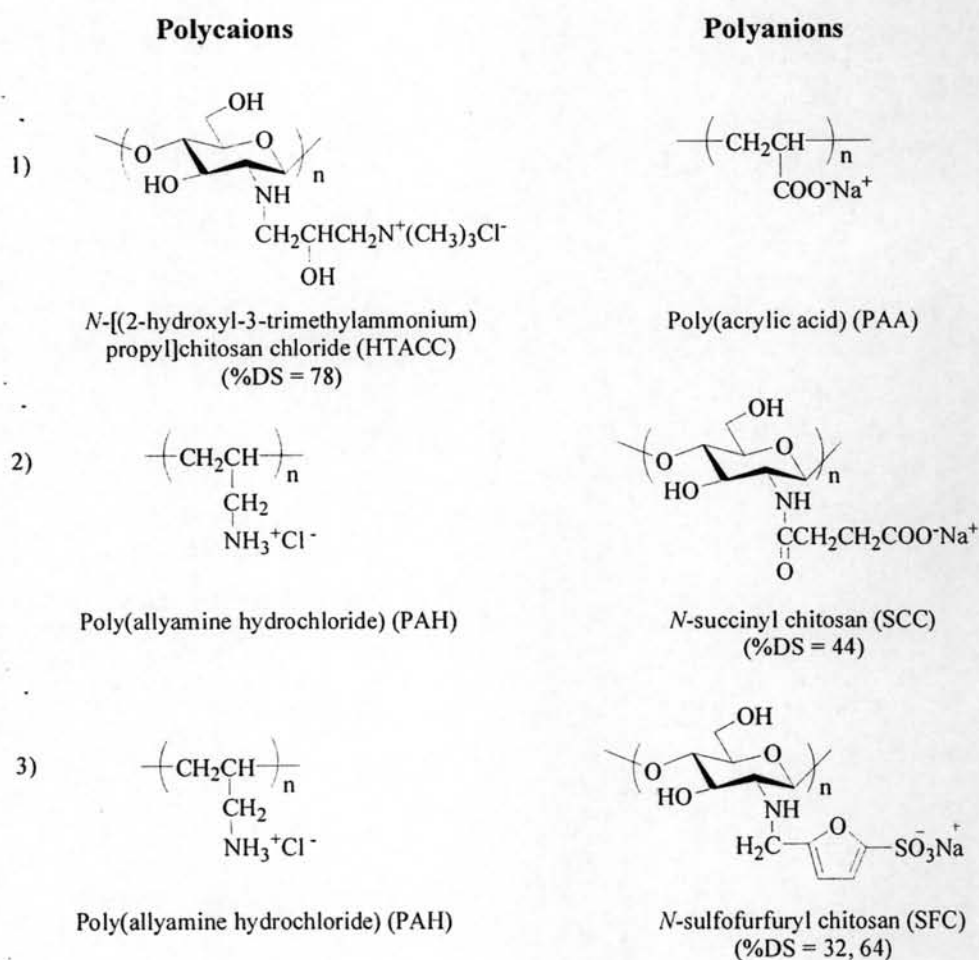


**Figure 4.9** Frequency shift of the quartz plate upon the adsorption of HTACC for 20 min as a function of HTACC concentration as determined by QCM using the conventional mode.

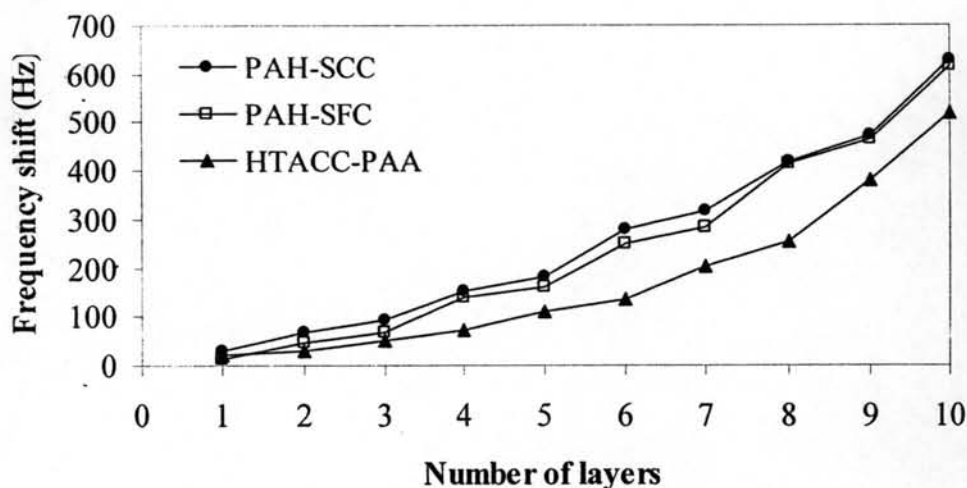
## 4.2 Multilayer Assembly

### 4.2.1 Growth of Multilayer Film

The conventional mode of QCM measurements was used to follow the multilayer formation on the gold-coated QCM plate by monitoring frequency change as a function of the number of depositions. Three polycation-polyanion pairs of polyelectrolytes were used for multilayer assembly: HTACC-PAA, PAH-SCC, and PAH-SFC. Their structures are illustrated in Scheme 4.1. It should be noted that all multilayer assembly was carried out in the presence of 0.5 M NaCl. Progressive increases in QCM frequency shift with the number of deposition steps (shown in Figure 4.10) evidently indicated a stepwise deposition of all three systems.



**Scheme 4.1** Polycations and polyanions used for multilayer assembly.



**Figure 4.10** Frequency shift (Hz) due to multilayer assembly on thiol-modified gold-coated QCM plate, obtained from QCM analysis as a function of the number of layers.

The QCM measurements in air using the conventional mode allow the dried mass of the deposited polyelectrolyte which is correlated to the thickness to be directly calculated from the Sauerbrey equation without having to take into account the swelling, frictional factor or over-adsorption that are usually encountered in the in situ mode. QCM is an extremely sensitive mass sensor, capable of weighing subnanogram levels. The piezoelectric quartz crystal changes its fundamental oscillation frequency ( $F_q$ ), as mass is deposited onto (or depleted from) the crystal surface in accordance with the Sauerbrey equation [64] in Eq. (4.1):

$$\Delta F = \frac{-2F_q^2 \Delta m}{A (\rho_q \mu_q)^{1/2}} \quad (4.1)$$

where  $\Delta F$  is the change in resonant frequency, resulting from the change due to adsorbed mass,  $\Delta m$ ,  $F_q$  is the fundamental resonant frequency of the quartz ( $5 \times 10^6$  Hz),  $A$  is the electrode area ( $0.3165 \text{ cm}^2$ ),  $\rho_q$  ( $2.65 \text{ g/cm}^3$ ) is the density of the quartz, and  $\mu_q$  is the shear modulus of the quartz ( $2.95 \times 10^6 \text{ N/cm}^2$ ). Substituting these

values in Eq. (4.2) for a one-sided adsorption on the QCM plate, we obtain the following relationship between adsorbed mass and frequency shift:

$$\Delta m \text{ (g)} = -5.60 \times 10^{-9} \Delta F \text{ (Hz)} \quad (4.2)$$

Assuming a rigid adsorbed layer, homogeneous surface coverage and the density of the polyion layers ( $\rho$ ) of 1.2 g/cm<sup>3</sup> [71], the thickness ( $d$ ) of the film (adsorbed on one side of the QCM plate,  $A = 0.3165 \text{ cm}^2$ ) can be estimated by substituting  $\rho dA$  for  $\Delta m$  in Eq. (4.3). The relationship between the thickness and the frequency shift can be expressed as follows:

$$d \text{ (nm)} = -0.147 \Delta F \text{ (Hz)} \quad (4.3)$$

The average frequency shifts ( $\Delta F_{av}$ ) and the corresponding bilayer thicknesses ( $db$ ) calculated from Eq. (4.3) are outlined in Table 4.5. Two average frequency shift values were reported.  $\Delta F_{av,odd}$  is an average value calculated from the shift between the odd layers (5, 7 and 9).  $\Delta F_{av,even}$  is an average value calculated from the shift between the even layers (6, 8 and 10). The results indicated that the thickness of multilayer film markedly increased as a function of degree substitution (%DS) of charged derivatives of chitosan, both SFC and HTACC. It should be underlined that the thiol-modified gold-coated QCM plate containing a mixed composition of COOH and OH groups represents a model of treated PET substrates, later it was used for multilayer assembly and cellular response studies.

The HTACC-PAA multilayer film built up from HTACC having 78%DS, was thicker than that built up from HTACC having 96%DS. This can be explained as a result of the incomplete substitution of *N*-[(2-hydroxyl-3-trimethylammonium) propyl] groups at the NH<sub>2</sub> position of chitosan. HTACC bears both the N(CH<sub>3</sub>)<sub>3</sub><sup>+</sup> and NH<sub>2</sub> groups. At the pH 7, the adsorption of HTACC on PAA was driven by both electrostatic interaction (N(CH<sub>3</sub>)<sub>3</sub><sup>+</sup> vs COO<sup>-</sup>) and H-bonding (NH<sub>2</sub> vs OH/NH<sub>2</sub>).

Having fewer number of  $N(CH_3)_3^+$ , HTACC with 78%DS had less tendency to adopt extended conformations than the HTACC with 96%DS. Its adsorption in the form of loops, tails and coils, especially those driven by H-bonding, was thus promoted. HTACC with less %DS would therefore yield a thicker adsorbed layer.

In the system of PAH-SCC, at pH 7, the adsorption of SCC on PAH layer was driven not only by H-bonding ( $NH_2$  vs  $OH/NH_2$ ) but also by electrostatic interaction ( $NH_3^+$  vs  $COO^-$ ). As a result of the incomplete substitution of *N*-succinyl groups at the  $NH_2$  position of chitosan (44% DS), SCC bears both  $COO^-$  and  $NH_2$  groups. Besides the train conformation, the polyelectrolytes were also in the form of loop, tail, or coil making the adsorbed layer to be thicker.

At pH 8, the adsorption of SFC on PAH layer was driven by both electrostatic interaction ( $NH_3^+$  vs  $SO_3^-$ ) and H-bonding ( $NH_2$  vs  $OH/NH_2$ ). Once again, the SFC having the %DS of 32% yield thicker adsorbed layer than SFC having %DS of 64%. With fewer number of  $SO_3^-$ , SCC with 32 %DS had less tendency to adopt extended conformations than the SCC with 64%DS. Its adsorption in the form of loops, tails and coils, especially those driven by H-bonding, was thus promoted.

From careful observations of the frequency shift, it is obvious that the shifts between the even layers are greater than those between the odd layers. This implies that there may be some changes of the internal structures of the odd layers (HTACC or PAH) due to relaxation or reformation toward the interface upon the deposition of the even layers (PAA, SCC or SFC), causing the multilayer to collapse and become more rigid. These changes were found to be highly dependent on the polyelectrolyte present in the outermost layer [72].

For further comparative studies, the multilayer films having a similar double layer thickness were chosen: HTACC-PAA assembled from HTACC with 78%DS, PAH-SCC assembled from SCC with 44%DS and PAH-SFC assembled from SFC with 64%DS.



**Table 4.5** Average frequency shift and bilayer thickness of three multilayer films assembled from charged derivatives of chitosan, as analyzed by QCM measurements using the conventional mode.

| Multilayer system   | $\Delta F_{av, odd}$ (Hz) | $db, odd$ (nm) | $\Delta F_{av, even}$ (Hz) | $db, even$ (nm) |
|---|---------------------------|----------------|----------------------------|-----------------|
| HTACC-PAA<br>(%DS = 78)                                   | 175                       | 25.7           | 177                        | 26.1            |
| HTACC-PAA<br>(%DS = 96)<br>(HTACC = 3 mg/mL) <sup>a</sup> | 14                        | 2.1            | 14                         | 2.1             |
| PAH-SCC<br>(%DS = 44)                                     | 145                       | 21.4           | 205                        | 30.0            |
| PAH-SFC<br>(%DS = 32)                                     | 294                       | 43.3           | 364                        | 53.5            |
| PAH-SFC<br>(%DS = 64)                                     | 152                       | 22.4           | 183                        | 26.9            |

a- the optimal concentration determined by Channasanon *et al.* [12]

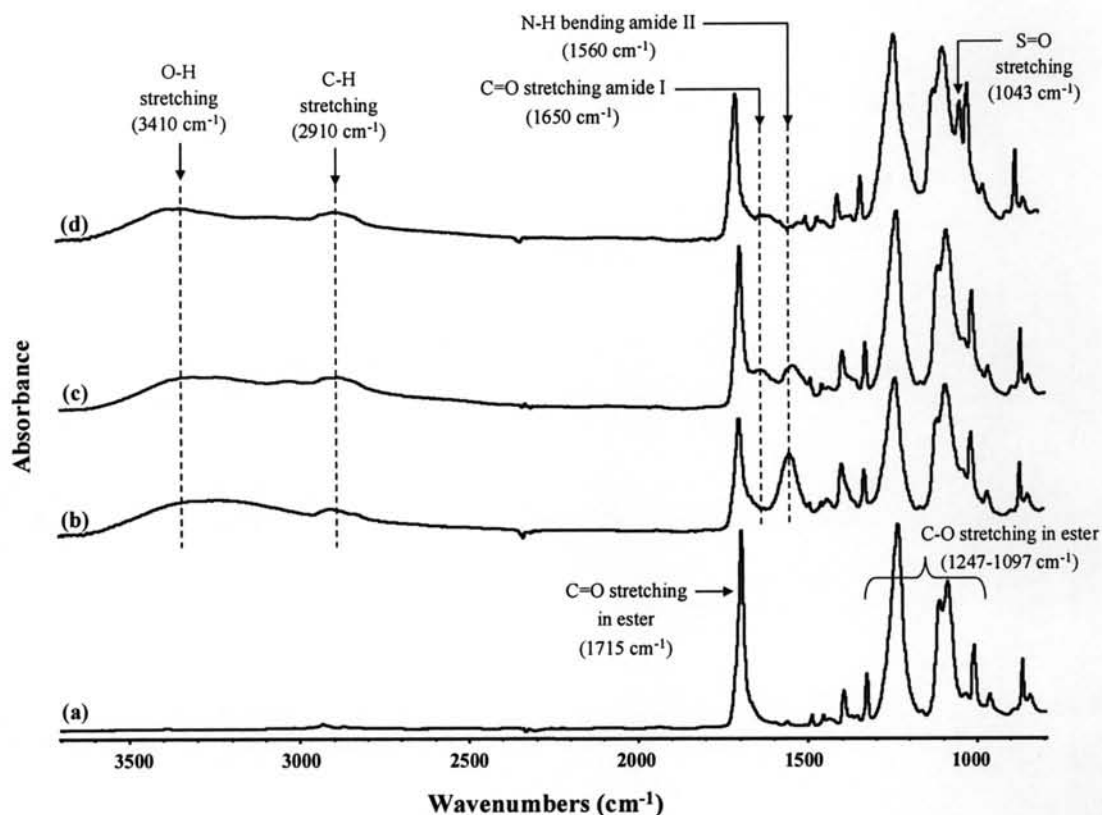
#### 4.2.2 Surface Coverage of Multilayer Film

Poly(ethylene terephthalate) (PET) has been recognized as a potential polymeric material for biomedical and biomaterials applications. However, due to the lack of bioactive functionality, a number of surface modification methods have been introduced to improve its favorable response to cells or proteins for specific applications. In this study, the plasma-treated PET plates which are commercially available were used as substrates for multilayer assembly. The treated PET substrate was pre-treated by basic hydrolysis prior to use in order to remove some organic dirt that might exist on the substrate and to enhance the hydrophilicity. After the pre-treatment, the water contact angle of the plasma-treated PET surface dropped from

81° to 64°. It should be noted that the virgin, unmodified PET surface usually possesses a water contact angle in the range of 77-80°. The basic hydrolysis has been proven to introduce carboxyl (COOH) and hydroxyl (OH) groups to the surface of PET [73]. We attempted to determine the presence of COOH groups on the surface of the treated PET substrates after the pre-treatment by ATR-FTIR analysis (Figure 4.11). However, this was unsuccessful possibly due to the modified layer being significantly thinner than the sampling depth of ATR-FTIR analysis (~ 1 µm). Nonetheless, we have verified the presence of COOH groups using the Toluidine blue O assay, a commonly known method for the determination of carboxyl group density [61]. The produced carboxyl groups on the surface of the plasma-treated PET plate can form a complex with toluidine blue O. The absorbance of the solution containing the desorbed complex was measured at 633 nm. The COOH content was obtained from a calibration plot of the optical density versus dye concentration (See Appendix B). The estimated carboxyl group density on the surface of treated PET substrate after the pre-treatment is  $1.46 \times 10^{-8}$  mol/cm<sup>2</sup>.

The coverage and functional groups of the multilayer films on the treated PET substrate were verified by ATR-FTIR analysis. Figure 4.11 shows ATR-FTIR spectra of treated PET substrates with multilayer films (16 layers). The signals due to carbonyl stretching (amide I) at 1650 cm<sup>-1</sup> of the glucosamine unit verifies the existence of chitosan in the multilayer film system of PAH-SCC and PAH-SFC while the signal from N-H bending of amide II is certainly enough to demonstrate the presence of SCC and HTACC in the PAH-SCC and HTACC-PAA multilayer films, respectively. The presence of absorption peaks at *ca.* 1192 and 1043 cm<sup>-1</sup> assigned to the O=S-O stretching and S=O stretching signifies the presence of SFC in the PAH-SFC multilayer film. Apparently, the broad peak over the region of O-H and N-H stretching in the range of 3750-2500 cm<sup>-1</sup> can be used as an indication of hydrogen bonding within the multilayer films. The presence of new signals that are characteristic peaks of polyelectrolytes in all samples implied that the thickness of the multilayer films reached the detection limit of ATR-FTIR technique. This result was consistent with the QCM data. According to QCM data, the thicknesses of 16 layers

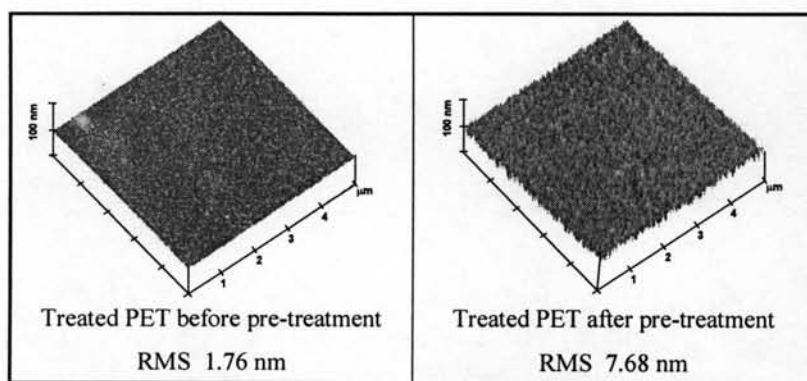
of three multilayer systems were close to  $\sim 200$  nm which is one fifth of the ATR-FTIR sampling depth.



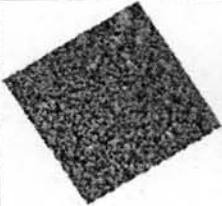
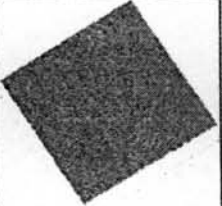
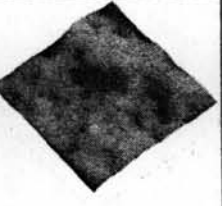
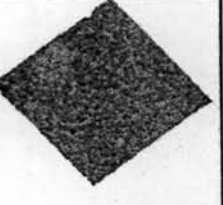

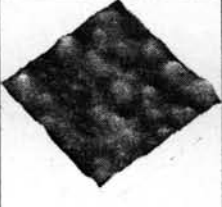

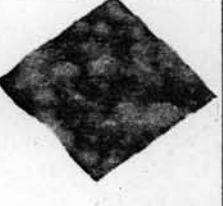


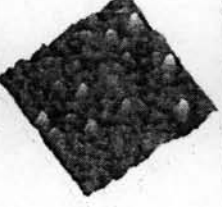
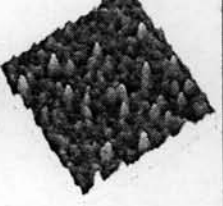
**Figure 4.11** ATR-FTIR spectra of treated PET substrates: (a) after pre-treatment and with multilayer films of (b) (HTACC-PAA)<sub>8</sub>, (c) (PAH-SCC)<sub>8</sub>, and (d) (PAH-SFC)<sub>8</sub>.

The coverage of the deposited multilayer films can be revealed from topographic images obtained by AFM analysis. AFM micrographs displayed in Figure 4.12 indicated that the treated PET substrates became rougher after the pre-treatment by basis hydrolysis. The root-mean-square roughness ( $R_{r.m.s.}$ ) increased from 1.76 to 7.68 nm. In the case of the HTACC-PAA and PAH-SCC multilayer systems, the surfaces became smoother after the deposition of 9-16 layers. It is understood that the assembly films grow homogeneously when the size of the roughness and the pores is far larger than molecular sizes of HTACC, PAA, PAH or

SCC and smaller than the average thickness of a single bilayer. This result was consistent with the previous conclusion that the deposition of polyelectrolyte layers has the ability to smooth-out a rough surface [74]. In the case of PAH-SFC multilayer system, the treated PET substrate was smoother after the deposition of 9 layers. The surface, however, became gradually rougher as the number of layer increased from 9 to 16 as shown in Figure 4.13.



**Figure 4.12** AFM images ( $5 \times 5 \mu\text{m}^2$ ) of treated PET substrates before and after pre-treatment.

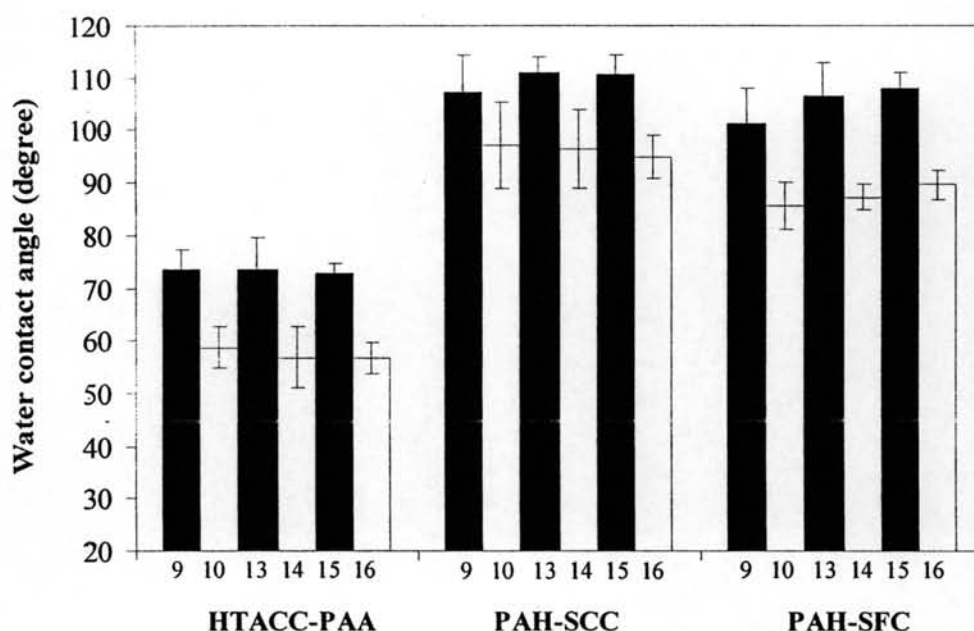
| Type of multilayer films | Number of Layers  |   |  |  |
|--------------------------|---|---|--|--|
|                          | 9   | 10  | 15   | 16   |
| HTACC-PAA                | <br>RMS 3.48 nm  | <br>RMS 2.80 nm  | <br>RMS 2.68 nm  | <br>RMS 2.19 nm   |
| PAH-SCC                  | <br>RMS 3.75 nm  | <br>RMS 4.75 nm  | <br>RMS 3.10 nm  | <br>RMS 3.73 nm   |
| PAH-SFC                  | <br>RMS 4.29 nm | <br>RMS 5.86 nm | <br>RMS 7.69 nm | <br>RMS 10.43 nm |

**Figure 4.13** AFM images ( $5 \times 5 \mu\text{m}^2$ ) of treated PET substrates with three multilayer systems: HTACC-PAA, PAH-SCC and PAH-SFC. The value listed under each micrograph is an average roughness.

#### 4.2.3 Stratification of Multilayer Film

If the concept of alternate adsorption is valid, the surface properties of the multilayer film should alternatively change. In other words, the multilayer film should be stratified. Water contact angle data shown in Figure 4.14 confirmed that the assembled film was stratified. The number appearing on the horizontal scale represents the number of depositions. If the number of layer is odd, the charge of the outermost layer is positive. If the number of layer is even, the charge of the outermost layer is negative. According to the calculation based on QCM analysis, each individual layer is apparently thicker than the sampling depth of contact angle measurement (a few Å) so that the wettability of the multilayer film should be strongly dictated by the last layer deposited and the influence of the underlying layers

should not be observed. The assembled films having the odd number of deposited layer (the positively charged surface) was clearly more hydrophobic than those having an even number of deposited layers (the negatively charged surface).



**Figure 4.14** Water contact angle of multilayer films assembled on treated PET substrates.

### 4.3 Cytocompatibility Test

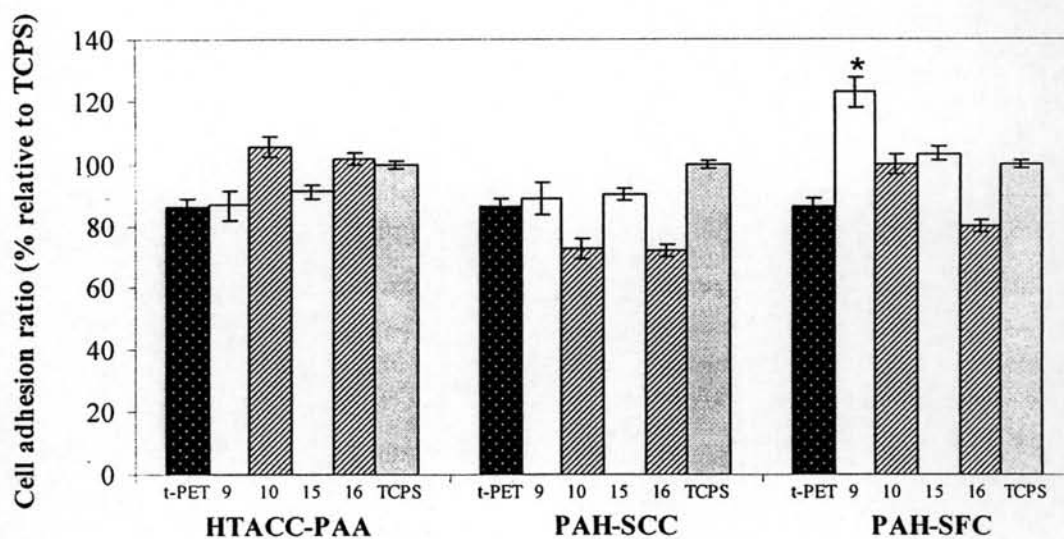
Previous study has demonstrated that the multilayer assembly of three pairs of polycation-polyanion (CHI-PSS at pH 4, PAH-SFC at pH 8 and HTACC-PAA at pH 7) on the plasma-treated PET substrates exhibited alternating protein adsorption. From a practical point of view, it is also important to determine whether such an alternating response is also realized by cells. Cell adhesion, spreading and migration on substrates are the first sequential reactions when coming into contact with a material surface, which is crucial for cell survival. The cellular behavior on biomaterials is an important factor for evaluation of the biocompatibility of a biomaterial [43].

In this research, the *in vitro* cytocompatibility of three multilayer systems (HTACC-PAA at pH 7, PAH-SCC at pH 7 and PAH-SFC at pH 8) on the treated PET substrates was carried out against L929 fibroblasts. To investigate the mitochondrial functions of the cultured L929, reduction of MTT reagent was used as an assay of mitochondrial redox activity. MTT reagent is a pale yellow substance that is reduced to a dark blue formazan product when incubating with viable cells by mitochondrial succinate dehydrogenase in complex II, which plays a critical role in both oxidative phosphorylation and tricarboxylic acid cycle. Therefore, the production of formazan can reflect the level of cell viability. The results (Figures 4.15 - 4.17) are reported in terms of the cell adhesion and proliferation ratio (% relative to TCPS) which is directly correlated to the number of viable cells. The value representing cell adhesion was detected after 12 h incubation. The values representing cell proliferation was detected after 48 h (2 days) and 96 h (4 days) incubations. The number appearing on the horizontal scale represented the number of deposition. If the number of layer is odd, the charge of the outermost layer is positive. If the number of layer is even, the charge of the outermost layer is negative.

Considering the HTACC-PAA system, the multilayer film having the even number of layer with PAA as the top layer seems to be more favorable for both cell adhesion and proliferation than those having the odd number of layer with HTACC as the top layer. The effectiveness of PAA in promoting positive cellular responses is equivalent to the tissue culture polystyrene (TCPS) which was used as a positive control. It is generally known that the cell membrane possesses negative charges. The opposite charges of HTACC should lead to a strong attraction with the cells and causes detrimental effect on the cells. The effect is more pronounced after 4 days of incubation (Figure 4.17). It has been previously reported that HTACC exhibit potent antibacterial activity [7,8]. That is why it has been used as an antibacterial agent for fibers.

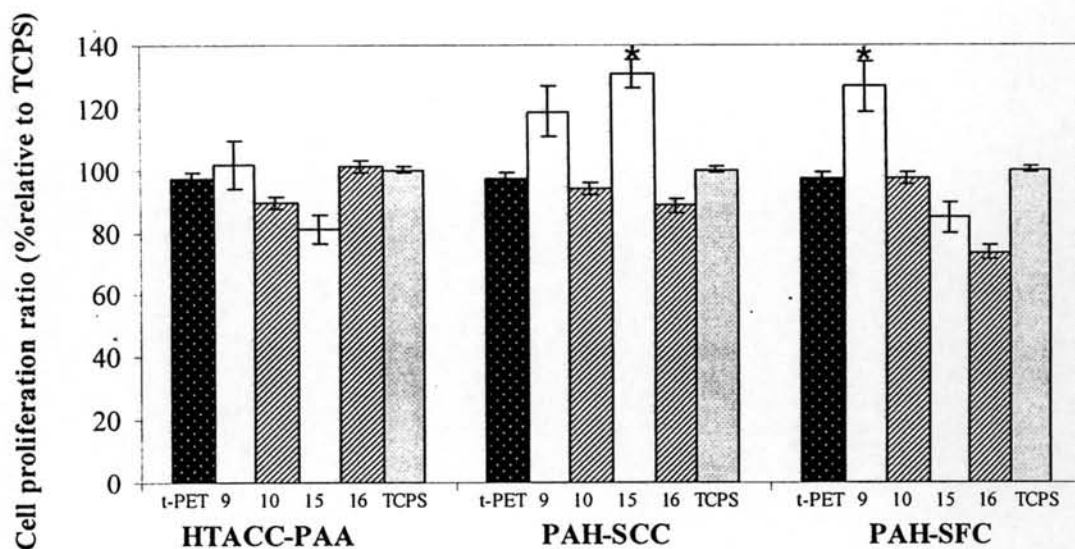
As opposed to the system of HTACC-PAA, the PAH-SCC multilayer films exhibit the opposite tendency. After 2 and 4 days of incubation, a significant improvement of cell adhesion was observed, especially when the number of layer was equal to 15 and PAH was the top layer. Unlike HTACC, PAH is a weak

synthetic polyelectrolyte that has been found to enhance early cell adhesion in the multilayer system of PSS/PAH [51] when it is the outermost layer of the film. The fact that SCC bears some negative charge, which is the same charge as the cell membrane, can explain why it is unfavorable for cell attachment. Evidently, the hydrophilic nature is not enough to counteract the charge repulsion. However, the same explanation cannot be applied with PAA. A similar trend was observed in the case of PAH-SFC system. In particular, the 9-layer multilayer film with PAH as the outermost layer gave significantly higher in both cell adhesion and proliferation than the treated PET substrate. The charge repulsion may also account for the inferior cellular responses of the multilayer films having SFC as the top layer. The cellular responses seem to be worse as a larger number of layers were deposited. There may be some influence from the increased roughness (See AFM data).

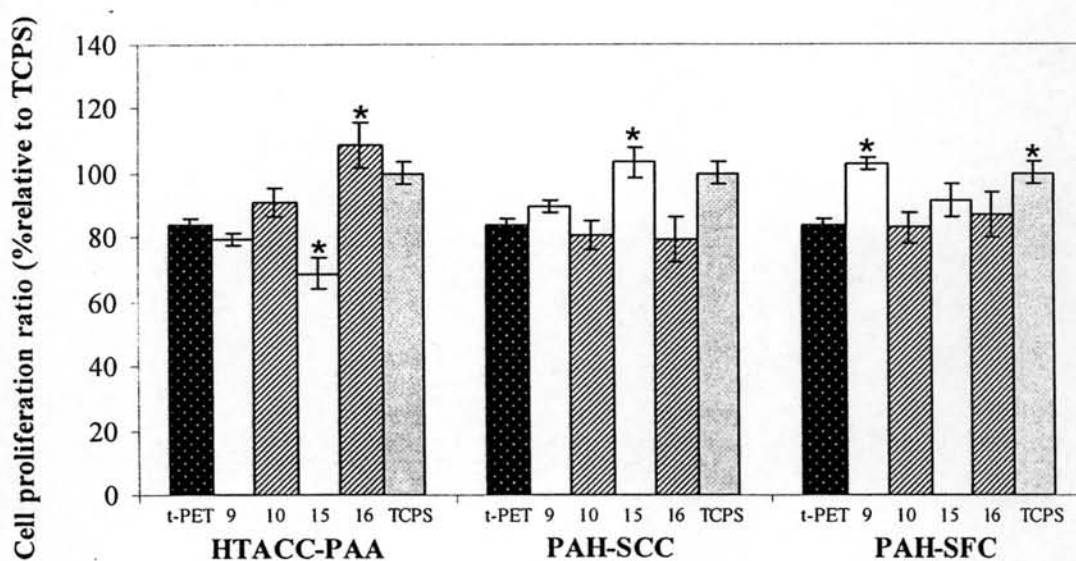


**Figure 4.15** Cell adhesion ratio (% relative to TCPS) of L929 cells at 12 h with a seeding density of  $5.0 \times 10^3$  cells/well on treated PET substrates with three multilayer systems: HTACC-PAA, PAH-SCC, PAH-SFC, and TCPS.





**Figure 4.16** Cell proliferation ratio (% relative to TCPS) of L929 cells at 2 days with a seeding density of  $5.0 \times 10^3$  cells/well on treated PET substrates with three multilayer systems: HTACC-PAA, PAH-SCC, PAH-SFC, and TCPS.



**Figure 4.17** Cell proliferation ratio (% relative to TCPS) of L929 cells at 4 days with a seeding density of  $5.0 \times 10^3$  cells/well on treated PET substrates with three multilayer systems: HTACC-PAA, PAH-SCC, PAH-SFC, and TCPS.

As a whole, these sets of data demonstrate that the degree of cytocompatibility of the multilayer films depends strongly on the polyelectrolyte used for the assembly process and the last layer deposited. Although none of the charged derivatives of chitosan promoted cell attachment and proliferation, it does not mean that they are useless. Materials that prevent cell adhesion may be useful for some biomedical applications.